MIXED MODE I + II INTERLAMINAR FRACTURE OF CARBON/EPOXY LAMINATES

A. B PEREIRA*, A. B. DE MORAIS*

***Department of Mechanical Engineering**
Universidade de Aveiro
Campus Santiago, 3810-193 Aveiro, Portugal

Abstract. This paper describes a study of the mixed mode I + II fracture of carbon/epoxy unidirectional and multidirectional specimens with symmetric, quasi-symmetric and markedly asymmetric legs. A beam model was developed for predicting the compliance and total strain energy release rate, G. Model predictions agreed well with three-dimensional finite element results for double cantilever beam, end-notched flexure and mixed mode bending tests. The mode mix was evaluated from a virtual crack closure technique limit analysis, which overcomes ambiguity in delaminations between differently oriented plies. Experimental specimen compliances were in good agreement with beam model predictions. Initiation critical strain energy release rates G_c were plotted against the mode II ratio G_{II}/G. Fracture loci of specimens with symmetric and quasi-symmetric legs had practically identical shapes, showing a linear G_c increase with $G_{II}/G > 25$ %. Moreover, G_c values of multidirectional specimens with quasi-symmetric and markedly asymmetric legs were very similar.

1. INTRODUCTION

Delamination is one of the most dangerous failure modes of high performance laminated composites. Numerous studies have been conducted on the characterisation of delamination resistance, especially on mode I and mode II fracture [1,2]. However, actual applications involve mixed mode loadings. Therefore, recent focus has been on mixed mode I + II fracture [2-13]. The mixed mode bending (MMB) test is considered the most appropriate for characterising interlaminar fracture resistance of unidirectional (UD) specimens over a wide range of mode combinations [2-4]. However, the MMB test is not suitable for experimental compliance calibration and inconsistencies in specimen compliance and toughness values have been reported when using beam models [3]. On the other hand, few studies have been conducted on multidirectional (MD) specimens [2-13], which are more representative of actual applications. Moreover, complicated problems exist in testing of MD specimens i.e intraply damage [5-9] and ambiguity in mode partitioning for delamination between differently oriented plies [13-15]. The approaches proposed to avoid this problem consist in adopting a characteristic length of crack extension [14] or using empirical mode partitioning equations that make compatible fracture test results from various types of specimens [15]

This paper reports a study of the mixed mode I + II interlaminar fracture of carbon/epoxy specimens [13]. Double cantilever beam (DCB), end-notched flexure (ENF) and MMB tests (Fig. 1) were performed on UD and MD specimens. Delamination interfaces analysed were 0/0, 0/45 and 0/90.

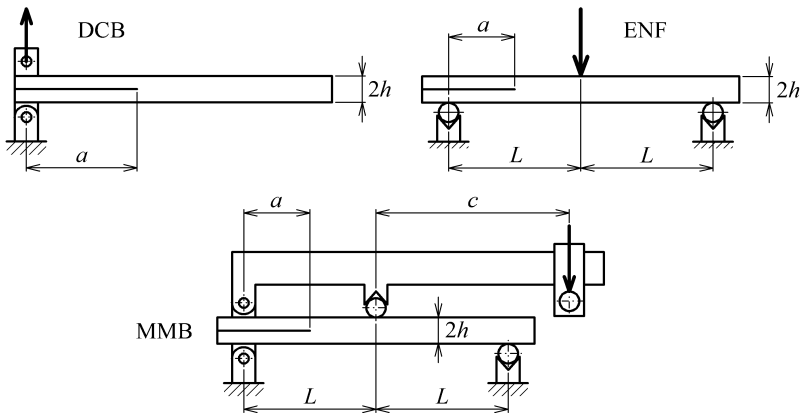

Fig. 1 - Schematic representation of the interlaminar fracture tests performed.

2. ANALYSIS

2.1. Beam model

The main objective of the beam model was to predict the compliance C and total strain energy release rate G of fracture specimens. As shown below, this model allowed accounting for the variability of specimen dimensions and elastic properties, and hence an efficient and accurate data reduction methodology. Initially, the main difficulty was to deal with asymmetric specimen legs and with crack tip rotations and deflections. It was assumed that such crack tip effects could be reasonably well taken into account in beam models by leg independent rotations and deflections. Consequently, different crack tip corrections $\Delta_{O,u}$ and $\Delta_{O,l}$ were used for the upper (u) and lower (l) legs of the DCB specimen (Fig. 2). The subscript 'O' for opening is adopted instead of 'I' because pure mode I does not occur with asymmetric legs.

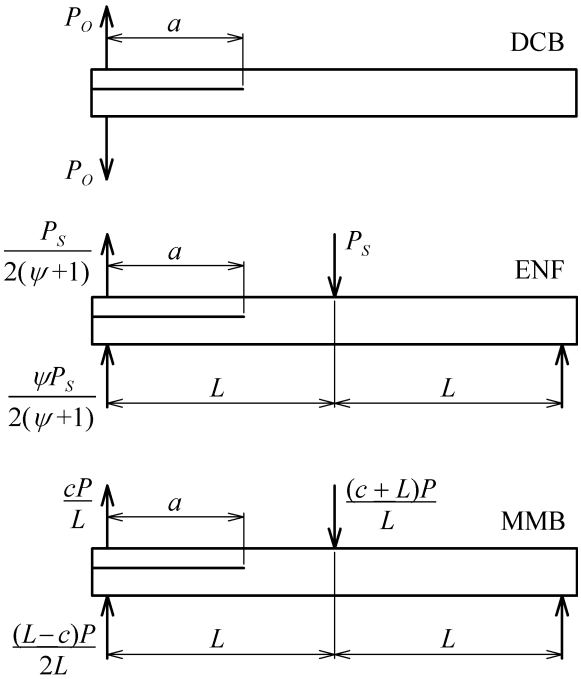

Fig. 2 - Forces in interlaminar fracture tests.

Therefore, neglecting transverse shear, the DCB specimen compliance is

$$C_O = \frac{4(\psi a_{O,u}^3 + a_{O,l}^3)}{b\psi E_u h_u^3} \tag{1}$$

where the equivalent crack lengths for each leg are

$$a_{O,u} = a + \Delta_{O,u}, \quad a_{O,l} = a + \Delta_{O,l} \tag{2}$$

b is the specimen width,

$$\psi = \frac{E_l}{E_u}\left(\frac{h_l}{h_u}\right)^3 \tag{3}$$

and h_u, h_l, E_u and E_l designate the thickness and Classical Lamination Theory (CLT) flexural modulus of the specimen legs. Finally, the Irwin-Kies relation gives

$$G_O = \frac{6P_O^2(\psi a_{O,u}^2 + a_{O,l}^2)}{b^2 \psi E_u h_u^3} \tag{4}$$

On the other hand, it is assumed that ENF specimen legs develop equal curvature by surface contact, thereby generating the equivalent leg point loads shown in Fig. 2. Beam analysis yields the compliance

$$C_S = \frac{(a_{S,u}^3 + \psi a_{S,l}^3)(\zeta - \psi - 1) + 2(\psi + 1)^2 L^3}{b\zeta(\psi + 1)^2 E_u h_u^3} + \frac{3L}{10bh\mu} \tag{5}$$

where *S* is used to designate "shear" fracture. The equivalent crack lengths are now

$$a_{S,u} = a + \Delta_{S,u}, \quad a_{S,l} = a + \Delta_{S,l} \tag{6}$$

and

$$\zeta = \frac{E}{E_u}\left(\frac{2h}{h_u}\right)^3 \tag{7}$$

while E and μ are the uncracked specimen flexural and transverse shear moduli, respectively. Eq. (5) assumes that $\mu_u \approx \mu_l \approx \mu$, which is realistic for most MD specimens. We have then

$$G_S = \frac{3P_S^2(a_{S,u}^2 + \psi a_{S,l}^2)(\zeta - \psi - 1)}{2b^2\zeta(\psi + 1)^2 E_u h_u^3} \tag{8}$$

Since the MMB test can be seen as the superposition of the DCB and ENF tests [3], we have

$$C = \frac{\delta}{P} = f_O C_O + f_S C_S \tag{9}$$

$$G = \left[f_O\left(\frac{G_O}{P_O^2}\right) + f_S\left(\frac{G_S}{P_S^2}\right)\right] P^2 \tag{10}$$

where P is the load applied and

$$f_O = \left[\frac{(2\psi + 1)c - L}{2(\psi + 1)L}\right]^2, \quad f_S = \left(\frac{c + L}{L}\right)^2 \tag{11}$$

It should mentioned that this beam model reduces exactly to the "corrected beam theory" [3] for standard UD specimens, except for the transverse shear term ($3L/10bh\mu$) in Eq. (5).

Where crack tip corrections are concerned, existing solutions for UD composites [16,17] where adapted to each specimen leg $i = u$ or l,

$$\Delta_{O,i} = h_i \sqrt{\frac{E_{x,i}}{11\mu_{xz,i}}\left[3 - 2\left(\frac{1.18\sqrt{E_{x,i}E_3}}{\mu_{xz,i} + 1.18\sqrt{E_{x,i}E_3}}\right)^2\right]} \tag{12}$$

$$\Delta_{S,i} = h_i \sqrt{\frac{E_{x,i}}{72\mu_{xz,i}}} \tag{13}$$

where x and z designate the length and thickness directions, respectively, $E_{x,i}$ is the leg flexural modulus, E_3 is the out-of-plane ply modulus and μ_{xz} is the transverse shear modulus obtained from expressions given in [18].

The beam model was applied to specimens obtained from a UD high strength carbon fibre (T300)/toughened epoxy prepreg (reference HS 160 REM) supplied by Texipreg. Nominal ply thickness t was 0.15 mm and ply properties E_1 = 130 GPa, E_2 = 8.2 GPa, ν_{12} = 0.27, μ_{12} = 4.1 GPa, ν_{23} = 0.41 were previously obtained. The specimen designations, stacking sequences and nominal thicknesses are given in table 1. All specimens had width b = 20 mm. It can be seen that MD45S and MD90S specimens have 0/45 and 0/90 delamination interfaces and quasi-symmetric legs. On the other hand, MD45A and MD90A specimens have identical delamination interfaces but markedly asymmetric legs. The main purpose of using the latter specimens was to check if they could avoid the spurious intraply cracking phenomenon. Furthermore, they enabled further evaluation of the mode partitioning approach described below.

Table 1 - Main characteristics of the specimens [13]. The starter delamination is designated by '//'.

Designation	Stacking sequence	$2h$ (mm)	a (mm)	L (mm)
UD	$[0_{14}//0_{14}]$	4.20	55	80
MD0S	$[(0_2/90)_6/0_2//(0_2/90)_6/0_2]$	6.00	70	100
MD45S	$[(0_2/90)_6/0_2//45/(0_2/90)_6/0_2]$	6.15	70	100
MD90S	$[(0_2/90)_6/0_2//90/(0_2/90)_6/0_2]$	6.15	70	100
MD45A	$[0_{10}//\pm45/0_{10}/\mp45/0_{10}]$	5.10	70	100
MD90A	$[0_{10}//90/0_{12}/90/0_{10}]$	5.10	70	100

2.2. FE analyses

The objectives of finite element (FE) analyses were to evaluate the beam model and to define the mode partitioning by the virtual crack closure technique (VCCT). 3D FE models were constructed in the ABAQUS® code using 8-node brick elements (Fig. 3) allowing laminate modelling. Mesh refinement was done near the crack tip and towards the specimen edges for VCCT application. Rigid body hinges were attached to the MMB specimen model for local load transmission. Rigid cylindrical surfaces simulated support and loading rollers.

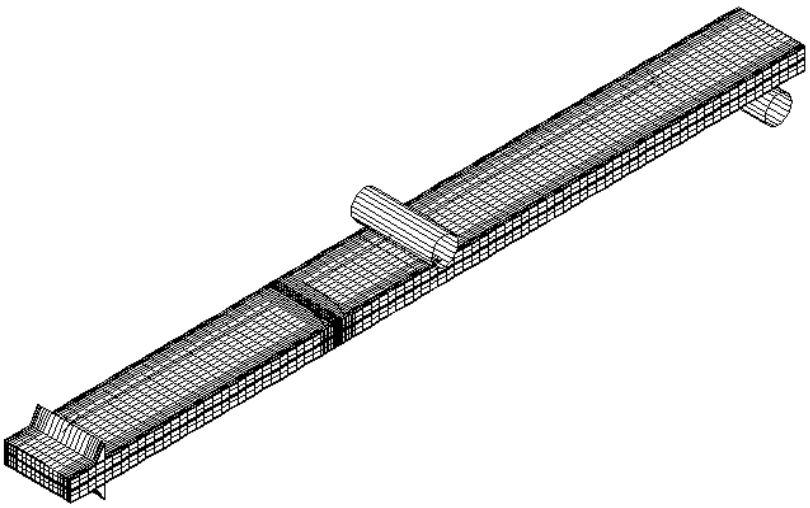

Fig. 3 – 3D model of a MMB specimen.

First, beam model compliance prediction equations (1), (5) and (9) were compared to FE values. Second, G values calculated from equations (4), (8) and (10) with FE loads were compared to VCCT values. Finally, VCCT mode partitioning was obtained for crack closure increments $\Delta a = t$ to $8t$, a range where G remained constant. In order to avoid loss of accuracy at high Δa values, the modified multi-element VCCT described in [10] was employed. The lever arm values used in MMB test simulations were (Fig. 1): c = 40, 62 and 120 mm for UD specimens; c = 50, 75 and 150 mm for MD0S, MD45S and MD90S specimens and c = 50 mm for MD45A and MD90A specimens.

Figs. 4 and 5 show the good performance of the beam model i.e. errors in C and G predictions relative to FE models were lower than 2 %. MMB configurations (a), (b) and (c) correspond to the decreasing c values mentioned above.

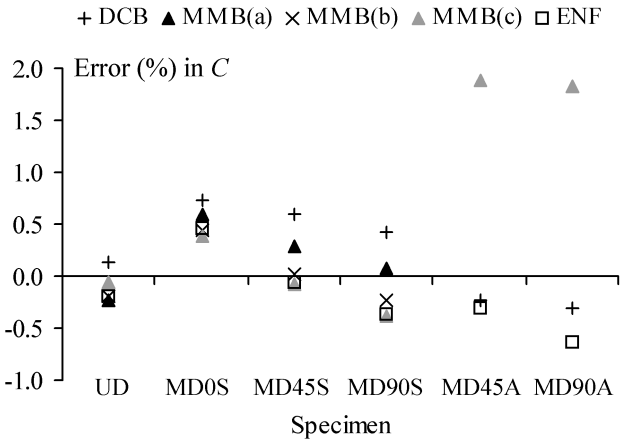

Fig. 4 - Errors of beam model compliance predictions relative to FE models [13].

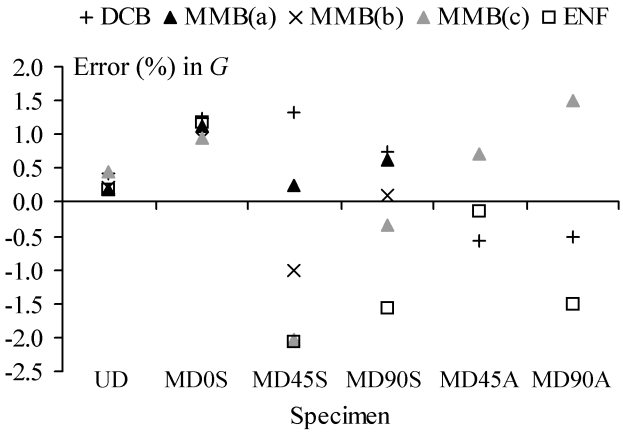

Fig. 5 - Errors of beam model total energy release rate predictions relative to FE models [13].

On the other hand, small but non-negligible mode mix dependence on the crack closure increment was detected in all MD MMB specimens and in MD45A and MD90A DCB specimens. Nevertheless, mode mix ratios rapidly tended to a limit for increasing Δa values (Fig. 6). This limit, obtained by extrapolation to $\Delta a = \infty$, was practically attained at $\Delta a = 8t$. Since fracture process zones associated to delaminations are quite large [15], the VCCT limit mode mix was adopted for experimental data analyses. In fact, this approach does not have any empirical basis and no inconvenient dependency on the crack extension. However, it has the disadvantage of requiring numerical analyses.

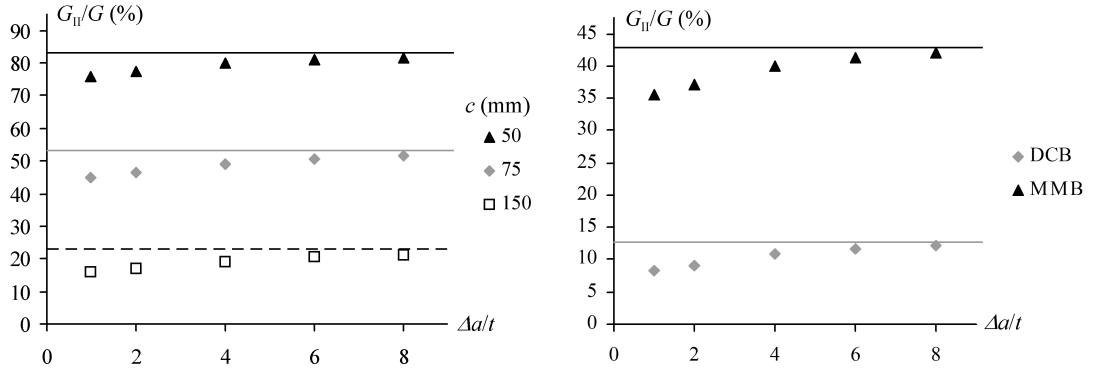

Fig. 6 - Influence of the crack closure increment on the mode mix of a) MD90S MMB b) MD90A DCB specimens. Lines represent extrapolated limits [13].

3. EXPERIMENTAL

3.1. Procedures

The specimens of table 1 were obtained from laminated plates manufactured by hot plate pressing. A 13 μm thick PTFE film was used to generate the starter crack. Specimens were cut from the plates by water jet and subjected to dimensional control. Machined Al alloy blocks were glued to DCB and MMB specimens for load transmission. Tests were conducted in a Shimadzu machine at 2 mm/min speed. A minimum of five specimens was tested in every case. The MMB fixture designed (Fig. 7) avoided the effect of its weight on toughness measurements by using a modified loading head [11] and a balancing weight at the end of the lever [13]. The limiting c values used were 40 to 280 mm for UD specimens and 50 to 350 mm for MD ones, enabling coverage of the $G_{II}/G \approx 12$ % to 85 % range.

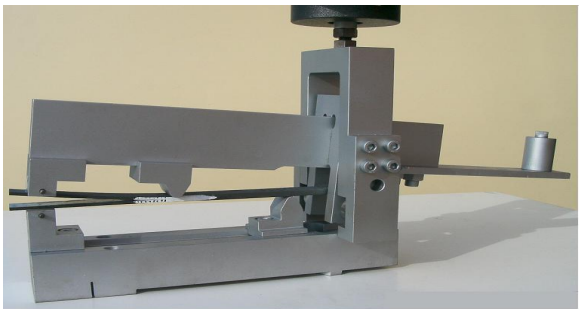

Fig. 7 - Picture of the MMB fixture [13].

Data reduction was performed with the above beam model by first using equations (1), (5) or (9) to back-calculate the specimen E_u flexural modulus. Other parameters were practically unaffected by specimen variability of elastic properties, while crack tip corrections only needed to be slightly modified for the true thickness e.g.

$$\Delta_{O,u} \approx (\Delta_{O,u})_{\text{nominal}} \frac{(h_u)_{\text{real}}}{(h_u)_{\text{nominal}}} \tag{14}$$

Then, G_c values where computed from initiation loads determined from the 5 % offset or maximum (5/M) load criteria. In fact, specimens exhibited very low non-linearity before the maximum load point.

On the other hand, additional FE analyses showed that the VCCT limit value was practically insensitive to specimen variability. In fact, the latter was small and affected in a quasi-identical way the properties

of specimen legs and uncracked area. Therefore, the data reduction methodology adopted avoided a large number of FE analyses of individual specimens.

3.2. Results and discussion

Fig. 8 shows typical load-displacement curves. In mode II dominated tests initiation was usually unstable and intraply damage was not observed. On the other hand, there was a minor instability in mode I dominated tests followed by a load increase associated to fibre bridging and intraply cracking of the off-axis interface ply (Fig. 9). Nevertheless, it was always possible to measure true interlaminar initiation G_c. Intraply damage was also observed in DCB and MMB tests of MD45A and MD90A specimens (Fig. 9), which thus were only useful for evaluating the mode partitioning approach.

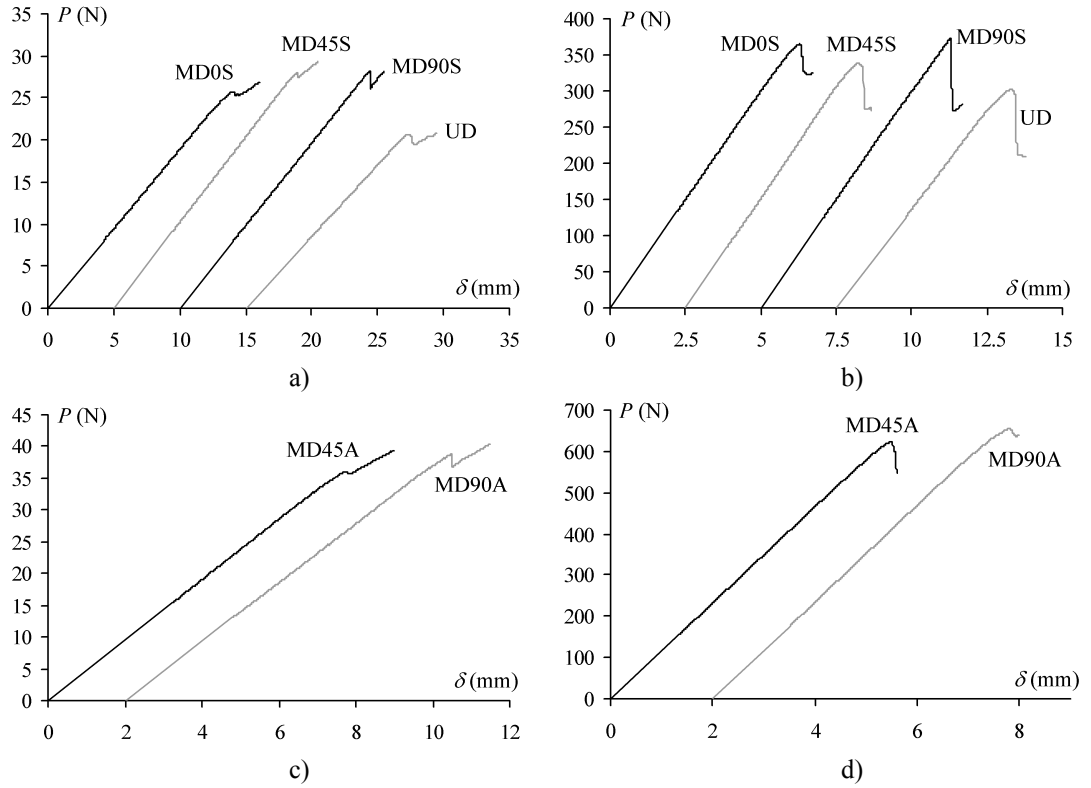

Fig. 8 - Typical load-displacement curves in a) high mode I ($G_{II}/G \approx 12$ %) MMB tests; b) high mode II ($G_{II}/G \approx 85$ %) MMB tests; c) DCB tests of MD45A and MD90A specimens; d) ENF tests of MD45A and MD90A specimens [13]. For clarity, some of the curves were offset

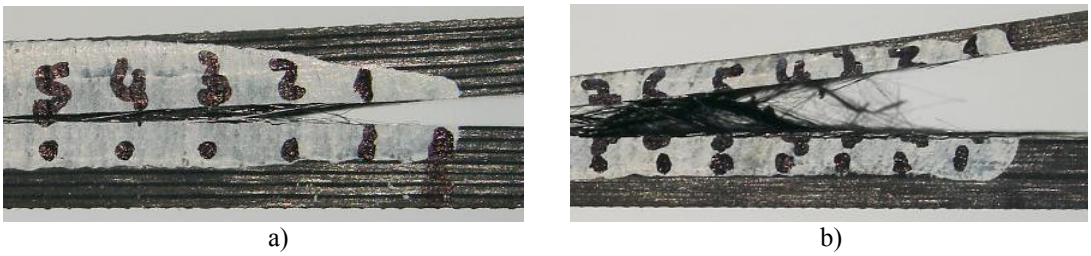

Fig. 9 - Picture of a) MMB MD90S specimen tested with a high mode I ($G_{II}/G \approx 12$ %) setup b) DCB MD45A specimen [13].

Fracture loci are plotted in Fig. 10. In all cases there was an initial mild increase of G_c with G_{II}/G, followed by linear growth for $G_{II}/G > 25$ %, approximately. Actually, G_c values were not significantly affected by the interface ply angle θ (Fig. 11). Moreover, results for MD45A and MD90A specimens

were consistent with those of MD45S and MD90S ones, respectively. Therefore, the proposed VCCT limit mode partitioning gave very realistic results and should be evaluated in future experimental studies on MD specimens.

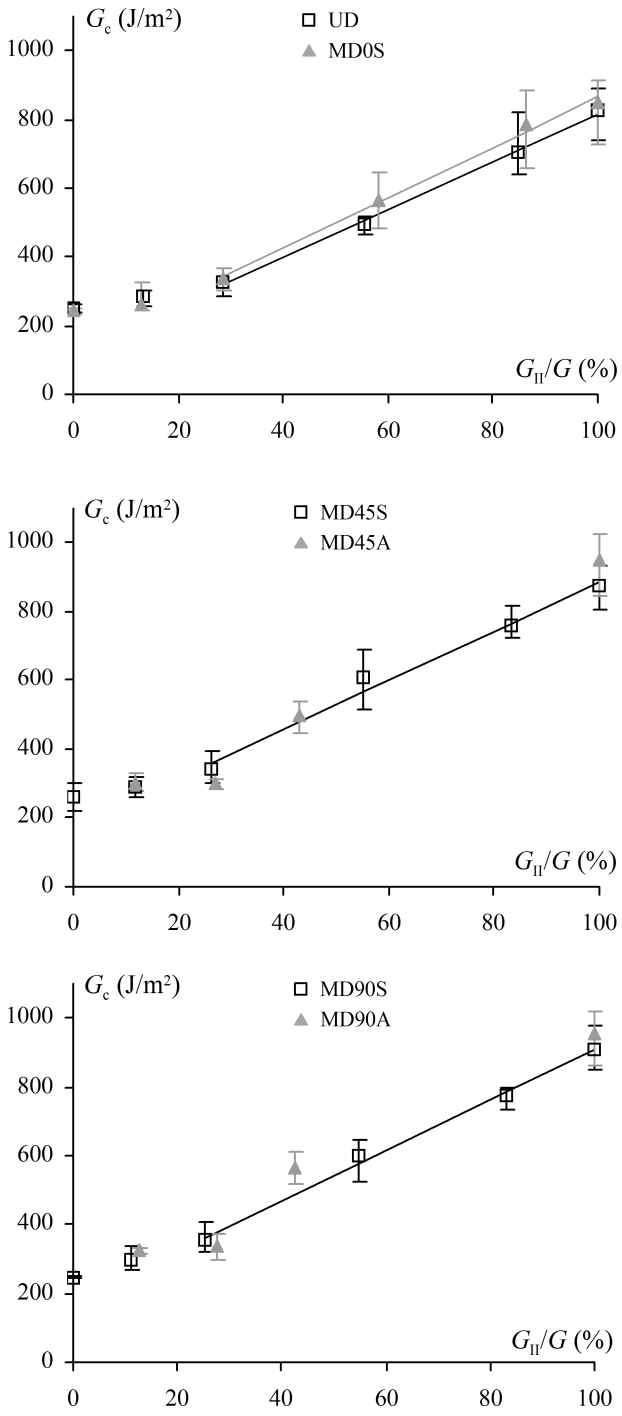

Fig. 10 - Average and scatter interval of measured G_c values. The plots include linear regression fits to the $G_{II}/G > 25$ % data of UD, MD0S, MD45S and MD90S specimens, as well as experimental data for MD45A and MD90A specimens [13].

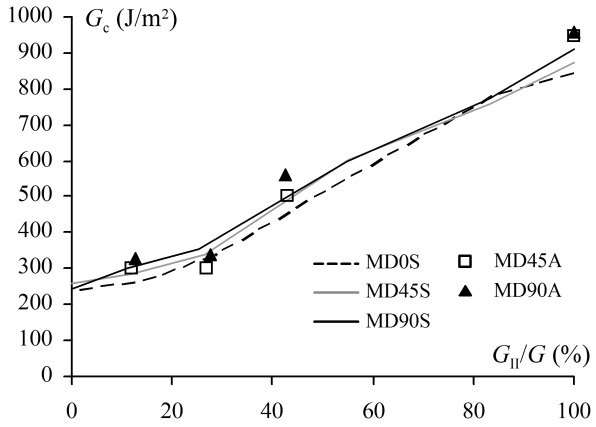

Fig. 11 - Comparison of average experimental G_c values for MD specimens [13].

4. CONCLUSIONS

A study was conducted on the mixed mode I + II fracture of carbon/epoxy unidirectional and multidirectional (MD) laminates. The specimens had symmetric, quasi-symmetric and markedly asymmetric legs. A beam model was developed for predicting the compliance and total strain energy release rate, G. Its predictions agreed well with three-dimensional finite element models of double cantilever beam (DCB), end-notched flexure (ENF) and mixed-mode bending (MMB). The beam model has the practical advantage of easily taking into account the variability of specimen dimensions and elastic properties.

As for mode partitioning, the virtual crack closure technique (VCCT) was applied with crack closure increments of the order of the ply thickness. A small but non-negligible dependence on the crack closure increment was seen for delamination between differently oriented plies. Nevertheless, VCCT mode mix results rapidly approached a limit, which was used for experimental data reduction because of the large fracture process zones usually associated to interlaminar fracture.

Plots of initiation G_c versus the G_{II}/G ratio had very similar shapes for specimens with symmetric legs. An initial mild increase of G_c with G_{II}/G was followed by linear growth for $G_{II}/G > 25$ %, approximately. In fact, G_c values of MD specimens were practically insensitive to the delamination interface. Moreover, results obtained with specimens having markedly asymmetric legs were consistent with the ones of quasi-symmetric legs. Therefore, the VCCT limit mode partitioning should be investigated in future studies on MD laminates. This approach does not require any empirical parameters, though numerical analyses are needed.

ACKNOWLEDGMENTS

This work was performed for the POCI/EME/57956/2004 research project, which is supported by the Portuguese Foundation for Science and Technology (FCT) and by the FEDER European Union fund. The authors thank the collaboration of Professors Marcelo F. de Moura (FEUP, Portugal), António G. Magalhães (ISEP, Portugal), António T. Marques (FEUP, Portugal) and Célia Novo (INEGI, Portugal).

REFERENCES

[1] Brunner, A.J, Flüeler, P., "Prospects in fracture mechanics of "engineering" laminates", Engng. Fract. Mech., 72, 899-908 (2005).

[2] Brunner, A.J., Blackman, B.R.K., Davies, P., "A status report on delamination resistance testing of polymer-matrix composites", EUROMECH 473 Colloquium, Porto, October 27-29, 2005, to be published in Engng. Fract. Mech.

[3] Reeder, J.R., "Refinements to the mixed-mode bending test for delamination toughness", J. Compos. Technol. Res., 25, 191-195 (2003).

[4] ASTM D 6671-04, "Standard test method for mixed mode I-mode II interlaminar fracture toughness of unidirectional fiber-reinforced polymer matrix composites".

[5] Polaha, J.J., Davidson, B.D., Hudson, R.C., Pieracci, A., "Effects of mode ratio, ply orientation and precracking on the delamination toughness of a laminated composite", J. Reinf. Plast. Compos., 15, 141-173 (1996).

[6] Choi, N.S., Kinloch, A.J., Williams, J.G., "Delamination fracture of multidirectional carbon-fibre/epoxy composites under mode I, mode II and mixed-mode I/II loading", J. Compos. Mater., 33, 73-100 (1999).

[7] Kim, B.W., Mayer, A.H., "Influence of fiber direction and mixed-mode ratio on delamination fracture toughness of carbon/epoxy laminates", Compos. Sci. Technol., 63, 695-713 (2003).

[8] Ozdil, F., Carlsson, L.A., "Beam analysis of angle-ply laminate mixed-mode bending specimens", Compos. Sci. Technol., 59, 937-945 (1999).

[9] Ozdil, F., Carlsson, L.A., "Characterization of mixed mode delamination growth in glass/epoxy composite cylinders", J. Compos. Mater., 34, 420-441 (2000).

[10] de Morais, A.B., Pereira, A.B., "Mixed mode I + II interlaminar fracture of glass/epoxy multidirectional laminates - Part 1: analysis", Compos. Sci. Technol., 66, 1889-1895 (2006).

[11] Pereira, A.B., de Morais A.B., "Mixed mode I + II interlaminar fracture of glass/epoxy multidirectional laminates - Part 2: experiments", Compos. Sci. Technol., 66, 1896-1902 (2006).

[12] de Morais, A.B., Pereira, A.B., "Interlaminar fracture of glass/epoxy multidirectional laminates under mixed mode I + II loading", Mech. Compos. Mater., 43, 349-366 (2007).

[13] Pereira, A.B., de Morais, A.B., "Mixed mode I + II interlaminar fracture of carbon/epoxy laminates", To be published in Composites Part A.

[14] Chow, W.T., Atluri, S.N., "Stress intensity factors as the fracture parameters for delamination crack growth in composite laminates", Composites, 28B, 375-384 (1997).

[15] Davidson, B.D., Bialaszewski, R.D., Sainath, S.S., "A non-classical, energy release rate based approach for predicting delamination in graphite reinforced laminated polymeric composites", Compos. Sci. Technol., 66, 1479-1496 (2006).

[16] Williams, J.G., "The fracture mechanics of delamination tests", J. Strain Analysis, 24, 207-214 (1989).

[17] Wang, J., Qiao, P., "Novel beam analysis of end notched flexure specimen for mode II fracture", Engng. Fract. Mech., 71, 219-231 (2004).

[18] Sun, C.T., Li, S., "Three-dimensional effective elastic constants for thick laminates", J. Compos. Mater., 22, 629-639 (1988).